doi: 10.15407/ujpe61.07.0597

O.R. BARAN, T.M. VERKHOLYAK

Institute for Condensed Matter Physics, Nat. Acad. of Sci. of Ukraine
(1, Svientsitskii Str., Lviv 79011, Ukraine)

TWO-DIMENSIONAL SPIN-1/2 $J_1 - J_1' - J_2$ HEISENBERG MODEL WITHIN JORDAN–WIGNER TRANSFORMATION

PACS 75.10.Jm, 75.40.Cx

The Jordan–Wigner transformation is applied to the spatially anisotropic spin-1/2 Heisenberg model on a square lattice with the nearest-neighbor and next-nearest-neighbor antiferromagnetic interactions. The transformed Hamiltonian describes the interacting spinless fermions that hop between neighbor sites in a gauge field. Using the mean-field-type approximation to both the direct interaction between fermions and the phase factors, which represent the gauge field, the problem is reduced to that concerning a free Fermi gas. Two types of antiferromagnetic ordering (the Néel and collinear ones) are considered. By calculating the ground-state energies, the phase transitions induced by the interaction frustration were analyzed.

K e y w o r d s: two-dimensional quantum spin models, frustrated models, fermionization.

1. Introduction

Due to the discovery of a variety of layered magnetic materials – in particular, $VOMoO_4$, Li_2VOSiO_4, Li_2VOGeO_4, $Pb_2VO(PO_4)_2$, and $SrZnVO(PO_4)_2$ – considerable attention is paid to the Heisenberg model on two-dimensional frustrated lattices (see works [1–8]). Those crystals are well described by the spin-1/2 Heisenberg model on a square lattice with the nearest-neighbor, J_1, and next-nearest-neighbor, J_2, interactions (the so-called $J_1 - J_2$ model). In three first above-mentioned substances, the both interactions are antiferromagnetic, whereas, in the last two, J_1 is ferromagnetic and J_2 is antiferromagnetic. The spin-1/2 $J_1 - J_2$ antiferromagnetic Heisenberg model on the square lattice was initially proposed in works [9–11], in which high-temperature cuprate superconductors were studied.

Besides the mentioned possibility for this frustrated spin-1/2 Heisenberg model with antiferromagnetic J_1 and J_2 interactions to serve as a basis for simulating real physical systems, it is also of purely theoretical interest, being one of the simplest two-dimensional models, in which the non-magnetic phases induced by competing interactions can arise [12]. In the case of weak J_2 interaction, the Néel antiferromagnetic (AF) ordering takes place in the ground state; otherwise, i.e. if the diagonal interactions J_2 are strong, the collinear stripe antiferromagnetic (CAF) ordering emerges.

The intermediate case with the largest competition between the interactions is very complicated for the analysis. This case corresponds to a magnetically disordered ground state with strong quantum correlations between the spins. The origin of this state and the number of phases between the ordered magnetic states remain a matter of discussion till now. Earlier, it was supposed that, in the non-magnetic phase, there is a crystal of valence bonds with a columnar [11, 13] or plaquette [14] ordering. However, the results of the variational resonance-valence-bond theory [15,16] and the tensor product state approach [17] testify in favor of a spin-liquid phase in the indicated region. Later results obtained in the framework of the density-matrix renormalization group method [18] and other numerical variational approaches [19, 20] revealed the topological character of the spin-liquid phase that arises in the $J_1 - J_2$ model. Recent researches distinguish two phases in the intermediate region: the topological spin-liquid phase (at $J_2/J_1 \leq 0.5$) and the crystalline phase of valence bonds with the plaquette [21] or columnar [22] symmetry (at $J_2/J_1 \geq 0.5$).

There are a lot of theoretical approaches to study quantum-mechanical spin systems with frustrations. For instance, the spin-1/2 $J_1 - J_2$ antiferromagnetic Heisenberg model on a square lattice was consid-

ered, in particular, by using the high-temperature expansion [5], density-matrix renormalization group method [18, 21], and quantum Monte-Carlo method [22], in the cluster approximation [24] and the variational approach [25], on the basis of Green's function theory [26–28], as well as using the methods of coupled clusters [29–31] and exact diagonalization [32, 33]. Each of the approaches has its shortcomings. For instance, the results of numerical methods strongly depend on the finite sizes of the system. On the other hand, the analytical methods often cannot describe strongly correlated disordered phases, which can arise at intermediate values of diagonal interactions. At the same time, while studying the low-dimensional quantum-mechanical models with competing interactions, the approaches, based on various versions of the Jordan–Wigner fermionization, may turn out to be rather efficient (see review [34]). An advantage of such analytical methods is the fact that the strongly correlated spin states can be described compactly in terms of fermionic excitations. For the first time, the one-dimensional Jordan–Wigner transformation, which makes it possible to change from spin operators to Fermi ones, was implemented for the one-dimensional spin-1/2 XY chain [35]. Later, various generalizations of fermionization onto two- and three-dimensional cases were intensively applied to the study of both the thermodynamic and dynamic properties of various systems [36–45].

An interesting generalization of the $J_1 - J_2$ model is a spatially anisotropic model, in which interactions between the nearest neighbors in orthogonal directions are different, and interactions J_2 are isotropic (the so-called $J_1 - J_1' - J_2$ model). This spin-1/2 $J_1 - J_1' - J_2$ Heisenberg model on a square lattice was introduced in work [46]. This model is of interest, first of all, because the model with the spatial anisotropy of interaction between both the nearest and the next-nearest neighbors (the $J_1 - J_1' - J_2 - J_2'$ model) turns out to be more adequate for the description of some magnetic materials mentioned above than the spatially isotropic model (see work [47]). In addition, the spatial anisotropy of at least one interaction substantially expands the class of real systems that can be simulated in the framework of the two-dimensional frustrated Heisenberg model. In particular, in work [48], the applicability of the $J_1 - J_1' - J_2$ Heisenberg model for the description of $(NO)[Cu(NO_3)_3]$ was demonstrated.

Like its spatially isotropic $J_1 - J_2$ counterpart, the spin-1/2 $J_1 - J_1' - J_2$ Heisenberg model on a square lattice has already been studied, by using several methods; in particular, the spin-wave expansion method [49, 50], the density-matrix renormalization group method [51], the effective-field method [52], in the variational approach [53], the method of coupled clusters [54], and the exact diagonalization method [55]. Some results obtained in the cited works will be mentioned below, while discussing our numerical results.

In this work, the method based on the Jordan–Wigner transformation is used to study the ground state of the spin-1/2 $J_1 - J_1' - J_2$ Heisenberg models on a square lattice. Here, we performed the Jordan–Wigner fermionization, which was proposed in work [56] for a two-dimensional Heisenberg model, but with the nearest-neighbor interaction only. In the mean-field-like approximation, similarly to what was done in works [37, 56], we consider two possible types of antiferromagnetic ordering. The thermodynamic functions are obtained, and the magnetic order parameter in the ground state is calculated. The results obtained are compared with the results of other methods.

2. Jordan–Wigner Fermionization. Mean-Field-Like Approximation

Let us consider a quantum spin-1/2 Heisenberg model with exchange interactions between the nearest, J_1 and J_1', and the next-nearest, J_2, neighbors on a square $N_x \times N_y$ lattice ($N_x \to \infty$, $N_y \to \infty$). The system is described by the Hamiltonian

$$
\begin{aligned}
&H = H_{XY} + H_Z,\\
&H_{XY} = \sum_{i=1}^{N_x}\sum_{j=1}^{N_y}\Big[J_1'(S_{i,j}^x S_{i+1,j}^x + S_{i,j}^y S_{i+1,j}^y) +\\
&+ J_1(S_{i,j}^x S_{i,j+1}^x + S_{i,j}^y S_{i,j+1}^y) +\\
&+ J_2(S_{i,j}^x S_{i+1,j+1}^x + S_{i,j}^y S_{i+1,j+1}^y +\\
&+ S_{i,j+1}^x S_{i+1,j}^x + S_{i,j+1}^y S_{i+1,j}^y)\Big],\\
&H_Z = \sum_{i=1}^{N_x}\sum_{j=1}^{N_y}\Big[J_1' S_{i,j}^z S_{i+1,j}^z + J_1 S_{i,j}^z S_{i,j+1}^z +\\
&+ J_2(S_{i,j}^z S_{i+1,j+1}^z + S_{i,j+1}^z S_{i+1,j}^z)\Big].
\end{aligned}
\tag{1}
$$

Here, for convenience, we separated the XY, H_{XY}, and Ising, H_Z, parts of the Heisenberg model. We

are interested in the case of frustrated interactions, when all of them are antiferromagnetic, i.e. $J_1 > 0$, $J_1' > 0$, and $J_2 > 0$. Without loss of generality let us put $J_1' \le J_1$.

Introducing the operators $S^{\pm}_{i,j} = S^x_{i,j} \pm \mathrm{i}S^y_{i,j}$, the Hamiltonian components H_{XY} and H_Z can be rewritten as follows:

$$H_{XY} = \frac{1}{2}\sum_{i=1}^{N_x}\sum_{j=1}^{N_y}\Big[J_1'(S^+_{i,j}S^-_{i+1,j} + S^+_{i+1,j}S^-_{i,j}) + \\ + J_1(S^+_{i,j}S^-_{i,j+1} + S^+_{i,j+1}S^-_{i,j}) + \\ + J_2(S^+_{i,j}S^-_{i+1,j+1} + S^+_{i+1,j+1}S^-_{i,j} + \\ + S^+_{i,j+1}S^-_{i+1,j} + S^+_{i+1,j}S^-_{i,j+1})\Big], \tag{2}$$

$$H_Z = \sum_{i=1}^{N_x}\sum_{j=1}^{N_y}\Big[J_1'\Big(S^+_{i,j}S^-_{i,j} - \frac{1}{2}\Big)\Big(S^+_{i+1,j}S^-_{i+1,j} - \frac{1}{2}\Big) + \\ + J_1\Big(S^+_{i,j}S^-_{i,j} - \frac{1}{2}\Big)\Big(S^+_{i,j+1}S^-_{i,j+1} - \frac{1}{2}\Big) + \\ + J_2\Big(S^+_{i,j}S^-_{i,j} - \frac{1}{2}\Big)\Big(S^+_{i+1,j+1}S^-_{i+1,j+1} - \frac{1}{2}\Big) + \\ + J_2\Big(S^+_{i,j+1}S^-_{i,j+1} - \frac{1}{2}\Big)\Big(S^+_{i+1,j}S^-_{i+1,j} - \frac{1}{2}\Big)\Big]. \tag{3}$$

It should be noted that the operators $S^+_{i,j}$ and $S^-_{i,j}$ at the same site satisfy the Fermi commutation relations $\{S^-_{i,j}, S^+_{i,j}\} = 1$ and $\{S^+_{i,j}, S^+_{i,j}\} = \{S^-_{i,j}, S^-_{i,j}\} = 0$; and, at different sites, the Bose commutation relations $[S^-_{i,j}, S^+_{l,n}] = = [S^+_{i,j}, S^+_{l,n}] = [S^-_{i,j}, S^-_{l,n}] = 0$.

Let us use the variant of the Jordan–Wigner transformation, which was proposed in work [56],

$$S^-_{i,j} = \mathrm{e}^{\mathrm{i}\varphi_{i,j}}d_{i,j}, \quad S^+_{i,j} = \mathrm{e}^{-\mathrm{i}\varphi_{i,j}}d^+_{i,j}, \tag{4}$$

$$\varphi_{i,j} = \sum_{l(\neq i)}\sum_{n(\neq j)}\mathrm{Im}\ln\Big[l - i + \mathrm{i}(n-j)\Big]d^+_{l,n}d_{l,n}. \tag{5}$$

Here, the coefficients $\varphi_{i,j}$ are chosen so that the operators $d^+_{i,j}$ and $d_{i,j}$ should satisfy the Fermi commutation relations both at the same site and at different sites: $\{d^+_{i,j}, d_{l,n}\} = \delta_{i,l}\delta_{j,n}$ and $\{d^+_{i,j}, d^+_{l,n}\} = = \{d_{i,j}, d_{l,n}\} = 0$.

On the basis of Eq. (4), let us present Hamiltonian (1) in the fermionic form [34, 37, 56, 57]:

$$H_{XY} = \frac{1}{2}\sum_{i=1}^{N_x}\sum_{j=1}^{N_y}\Big[J_1'd^+_{i,j}\mathrm{e}^{\mathrm{i}(\varphi_{i+1,j}-\varphi_{i,j})}d_{i+1,j} + \\ + J_1'd^+_{i+1,j}\mathrm{e}^{\mathrm{i}(\varphi_{i,j}-\varphi_{i+1,j})}d_{i,j} + \\ + J_1d^+_{i,j}\mathrm{e}^{\mathrm{i}(\varphi_{i,j+1}-\varphi_{i,j})}d_{i,j+1} + \\ + J_1d^+_{i,j+1}\mathrm{e}^{\mathrm{i}(\varphi_{i,j}-\varphi_{i,j+1})}d_{i,j} + \\ + J_2d^+_{i,j}\mathrm{e}^{\mathrm{i}(\varphi_{i+1,j+1}-\varphi_{i,j})}d_{i+1,j+1} + \\ + J_2d^+_{i+1,j+1}\mathrm{e}^{\mathrm{i}(\varphi_{i,j}-\varphi_{i+1,j+1})}d_{i,j} + \\ + J_2d^+_{i,j+1}\mathrm{e}^{\mathrm{i}(\varphi_{i+1,j}-\varphi_{i,j+1})}d_{i+1,j} + \\ + J_2d^+_{i+1,j}\mathrm{e}^{\mathrm{i}(\varphi_{i,j+1}-\varphi_{i+1,j})}d_{i,j+1}\Big], \tag{6}$$

$$H_Z = \sum_{i=1}^{N_x}\sum_{j=1}^{N_y}\Big[J_1'\Big(d^+_{i,j}d_{i,j} - \frac{1}{2}\Big)\Big(d^+_{i+1,j}d_{i+1,j} - \frac{1}{2}\Big) + \\ + J_1\Big(d^+_{i,j}d_{i,j} - \frac{1}{2}\Big)\Big(d^+_{i,j+1}d_{i,j+1} - \frac{1}{2}\Big) + \\ + J_2\Big(d^+_{i,j}d_{i,j} - \frac{1}{2}\Big)\Big(d^+_{i+1,j+1}d_{i+1,j+1} - \frac{1}{2}\Big) + \\ + J_2\Big(d^+_{i,j+1}d_{i,j+1} - \frac{1}{2}\Big)\Big(d^+_{i+1,j}d_{i+1,j} - \frac{1}{2}\Big)\Big]. \tag{7}$$

The XY part of the Hamiltonian corresponds to spinless fermions on a square lattice, which jump between the nearest and next-nearest sites in the gauge field [56]. The part H_Z describes the direct interaction between the fermions. It should be noted that, unlike the XY chain, the fermionic representation of the two-dimensional XY model already contains the interaction between the fermions, which is hidden in the phase factors.

For the further consideration of the fermionic Hamiltonian (Eqs. (6) and (7)), an approximation of the mean-field type [34, 56, 59] adapted to the model with the next-nearest-neighbor interaction (see details in works [57, 58]) will be used. In particular, for the phase factors $\exp(\pm\mathrm{i}\varphi_{i,j})$ in Hamiltonian (6), the operators of fermion number $n_{i,j} = d^+_{i,j}d_{i,j}$ are substituted by their average values. In this approximation, if the total magnetization of the lattice equals zero, the part XY of the Hamiltonian transforms [34, 56, 59] into a Hamiltonian for a system of spinless fermions that move in a uniform magnetic field with the flux $\Phi_0 = \pi$ through an elementary square plaquette. Accordingly, the flux through a triangular plaquette (its two sides are the orthogonal basis vectors of the lattice) is equal to $\pi/2$ by analogy with work [60].

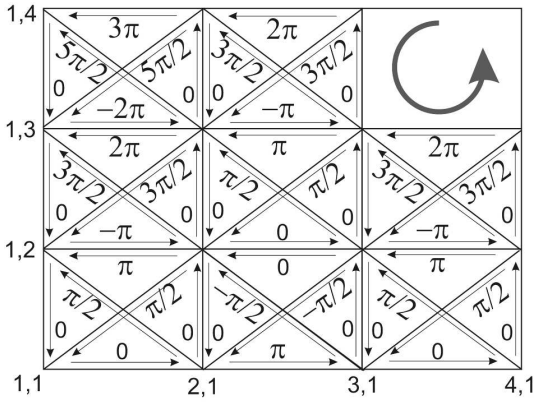

a

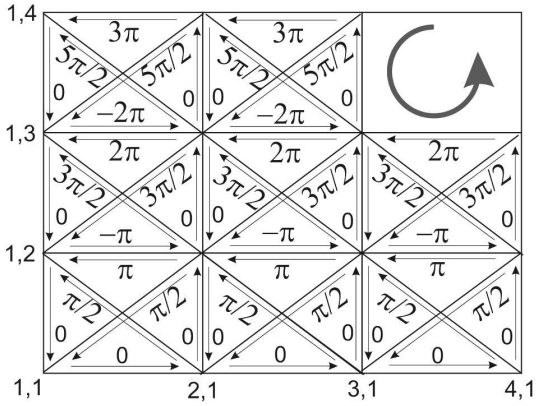

b

Fig. 1. Choice of the phase difference $\varphi_{i,j} - \varphi_{l,n}$, which provides the flux $\Phi_0 = \pi$ of the magnetic field through an elementary square plaquette and a flux of $\pi/2$ through half a plaquette in the form of a triangle, whose sides are the orthogonal basis vectors of the lattice in the cases of Néel (*a*) and collinear (*b*) orderings

The fermionic representation (6), as well as its mean-field approximation, is invariant with respect to the gauge transformation. Therefore, in case of Néel antiferromagnetic ordering, we may, for convenience, calibrate the vector potential, as it was done in works [34, 56, 59] (see Fig. 1, *a*). Then, in the mean-field approximation, Eq. (6) can be rewritten in the form

$$H_{XY}^{\mathrm{AF}} = \frac{1}{2}\sum_{i=1}^{N_x}\sum_{j=1}^{N_y}\Big\{J_1\left(d_{i,j}^{+}d_{i,j+1} + d_{i,j+1}^{+}d_{i,j}\right) +$$

$$+ J_1'(-1)^{i+j}\left(d_{i,j}^{+}d_{i+1,j} + d_{i+1,j}^{+}d_{i,j}\right) -$$

$$- \mathrm{i}J_2(-1)^{i+j}\left(d_{i,j}^{+}d_{i+1,j+1} - d_{i+1,j+1}^{+}d_{i,j} +\right.$$

$$\left. + d_{i,j+1}^{+}d_{i+1,j} - d_{i+1,j}^{+}d_{i,j+1}\right)\Big\}. \tag{8}$$

In the case of collinear stripe antiferromagnetic ordering, it is convenient to gauge the potential following the scheme exhibited in Fig. 1, *b*. Then, we obtain Eq. (6) in the mean-field approximation, but in a form that is a little different from expression (8):

$$H_{XY}^{\mathrm{CAF}} = \frac{1}{2}\sum_{i=1}^{N_x}\sum_{j=1}^{N_y}\Big\{J_1\Big(d_{i,j}^{+}d_{i,j+1} + d_{i,j+1}^{+}d_{i,j}\Big) -$$

$$- J_1'(-1)^{j}\Big(d_{i,j}^{+}d_{i+1,j} + d_{i+1,j}^{+}d_{i,j}\Big) +$$

$$+ \mathrm{i}J_2(-1)^{j}\Big(d_{i,j}^{+}d_{i+1,j+1} - d_{i+1,j+1}^{+}d_{i,j} +$$

$$\left. + d_{i,j+1}^{+}d_{i+1,j} - d_{i+1,j}^{+}d_{i,j+1}\Big)\right\}. \tag{9}$$

For the four-fermionic terms in H_Z (7), the used mean-field-like approximation (see works [34, 37, 56, 59]) reads

$$d_{i,j}^{+}d_{i,j}d_{l,n}^{+}d_{l,n} \to d_{i,j}^{+}d_{i,j}\langle d_{l,n}^{+}d_{l,n}\rangle +$$

$$+ \langle d_{i,j}^{+}d_{i,j}\rangle d_{l,n}^{+}d_{l,n} - \langle d_{i,j}^{+}d_{i,j}\rangle\langle d_{l,n}^{+}d_{l,n}\rangle. \tag{10}$$

Here, only the correlation of fermions at identical sites are taken into account.

In the case of Néel antiferromagnetic ordering, when the magnetizations of sublattices m_A^{AF} and m_B^{AF} are equal by magnitude, but opposite by sign, and the lattice is split into sublattices so that $m_A^{\mathrm{AF}} = \langle S_{i,j}^z\rangle = \langle d_{i,j}^{+}d_{i,j}\rangle - \frac{1}{2} = \langle S_{i+1,j+1}^z\rangle = ... = -m_B^{\mathrm{AF}} = -\langle S_{i+1,j}^z\rangle = -\langle d_{i+1,j}^{+}d_{i+1,j}\rangle + \frac{1}{2} = -\langle S_{i,j+1}^z\rangle = ...)$, we obtain

$$H_Z^{\mathrm{AF}} = -2\tilde{J}m_A^{\mathrm{AF}}\sum_{i=1}^{N_x}\sum_{j=1}^{N_y}(-1)^{i+j}d_{i,j}^{+}d_{i,j} +$$

$$+ \tilde{J}N_xN_y\left(m_A^{\mathrm{AF}}\right)^2. \tag{11}$$

Here, the notation $\tilde{J} = J_1' + J_1 - 2J_2$ is used. Note that, while deriving relation (11), as well as some other ones given below, the periodic boundary conditions were applied.

In the case of stripe-like antiferromagnetic ordering at $J_1' \le J_1$, i.e. when the magnetizations of sublattices are $m_A^{\mathrm{CAF}} = \langle S_{i,j}^z\rangle = \langle d_{i,j}^{+}d_{i,j}\rangle -$

$-\frac{1}{2} = \langle S^z_{i+1,j}\rangle = ... = -m_B^{\rm CAF} = -\langle S^z_{i,j+1}\rangle = = -\langle S^z_{i+1,j+1}\rangle = ...$, we have

$$H_Z^{\rm CAF} = 2\tilde{J}' m_A^{\rm CAF} \sum_{i=1}^{N_x}\sum_{j=1}^{N_y} (-1)^j d^+_{i,j} d_{i,j} - - \tilde{J}' N_x N_y (m_A^{\rm CAF})^2. \quad (12)$$

Here, $\tilde{J}' = J_1' - J_1 - 2J_2$. Note that we accepted N_y in expression (12) to be an even number. For odd N_y, the Hamiltonian $H_Z^{\rm CAF}$ also includes a term (see work [58]), which is infinitesimally small in the thermodynamic limit. Therefore, it is omitted hereafter.

After changing in Eqs. (8), (11) and (9), (12) to the momentum space ($d_{i,j} = \frac{1}{\sqrt{N_x N_y}} \times \times \sum_{q_x,q_y} {\rm e}^{{\rm i}(q_x i + q_y j)} d_{q_x,q_y}$, $d^+_{i,j} = \frac{1}{\sqrt{N_x N_y}} \times \times \sum_{q_x,q_y} {\rm e}^{-{\rm i}(q_x i + q_y j)} d^+_{q_x,q_y}$), we obtain the Hamiltonian $H = H_{XY} + H_Z$ for the Heisenberg model in the cases of ordering that were mentioned above:

$$H^{\rm AF} = \sum_{q_x,q_y} \Big\{ \Big[-{\rm i}J_1' \sin q_x + 2J_2 \cos q_x \sin q_y - 2m_A^{\rm AF}\tilde{J}\Big] \times \times d^+_{q_x,q_y} d_{q_x-\pi,q_y-\pi} + J_1 \cos q_y d^+_{q_x,q_y} d_{q_x,q_y} \Big\} + + \tilde{J} N_x N_y (m_A^{\rm AF})^2, \quad (13)$$

$$H^{\rm CAF} = \sum_{q_x,q_y} \Big\{ \Big[-J_1' \cos q_x + 2{\rm i}J_2 \sin q_x \sin q_y + 2m_A^{\rm CAF}\tilde{J}'\Big] \times \times d^+_{q_x,q_y} d_{q_x,q_y-\pi} + J_1 \cos q_y\, d^+_{q_x,q_y} d_{q_x,q_y} \Big\} - - \tilde{J}' N_x N_y (m_A^{\rm CAF})^2. \quad (14)$$

Here, the summation is carried out over the first Brillouin zone.

Hamiltonian (13) can be written in the matrix form,

$$H^{\rm AF} = {\sum_{\mathbf{q}}}' (d^+_{q_x,q_y}\ d^+_{q_x-\pi,q_y-\pi}) \times \times \begin{pmatrix} C_{11}^{\rm AF} & C_{12}^{\rm AF} \\ (C_{12}^{\rm AF})^* & -C_{11}^{\rm AF} \end{pmatrix} \begin{pmatrix} d_{q_x,q_y} \\ d_{q_x-\pi,q_y-\pi} \end{pmatrix} + \tilde{J} N_x N_y (m_A^{\rm AF})^2, \quad (15)$$

where the notations $C_{11}^{\rm AF} = J_1 \cos q_y$ and $C_{12}^{\rm AF} = = -2m_A^{\rm AF}\tilde{J} + 2J_2 \cos q_x \sin q_y - {\rm i}J_1' \sin q_x$ are used, and the primed sum sign means that $\mathbf{q}$ belongs to the region $-\pi \le q_y \le \pi$, $-\pi + |q_y| \le q_x \le \pi - |q_y|$.

Analogously, Hamiltonian (14) can also be expressed in the matrix form:

$$H^{\rm CAF} = {\sum_{\mathbf{q}}}'' (d^+_{q_x,q_y}\ d^+_{q_x,q_y-\pi}) \times \times \begin{pmatrix} C_{11}^{\rm CAF} & C_{12}^{\rm CAF} \\ (C_{12}^{\rm CAF})^* & -C_{11}^{\rm CAF} \end{pmatrix} \begin{pmatrix} d_{q_x,q_y} \\ d_{q_x,q_y-\pi} \end{pmatrix} - \tilde{J}' N_x N_y (m_A^{\rm CAF})^2, \quad (16)$$

where $C_{11}^{\rm CAF} = J_1 \cos q_y$, $C_{12}^{\rm CAF} = 2m_A^{\rm CAF}\tilde{J}' - J_1' \cos q_x + + 2{\rm i}J_2 \sin q_x \sin q_y$, and two primes near the sum sign mean that $\mathbf{q}$ belongs to the upper half of the first Brillouin zone.

The quadratic forms (15) and (16) can be reduced to the diagonal form, by using the Bogolyubov canonical transformation, so that

$$H^{\rm AF} = {\sum_{\mathbf{q}}}' \lambda_{\mathbf{q}}^{\rm AF} \left[\beta^+_{\mathbf{q}}\beta_{\mathbf{q}} - \alpha^+_{\mathbf{q}}\alpha_{\mathbf{q}}\right] + + \tilde{J} N_x N_y (m_A^{\rm AF})^2, \quad (17)$$

$$H^{\rm CAF} = {\sum_{\mathbf{q}}}'' \lambda_{\mathbf{q}}^{\rm CAF} \left[\eta^+_{\mathbf{q}}\eta_{\mathbf{q}} - \gamma^+_{\mathbf{q}}\gamma_{\mathbf{q}}\right] - - \tilde{J}' N_x N_y (m_A^{\rm CAF})^2, \quad (18)$$

where ($\beta^+_{\mathbf{q}}$, $\alpha^+_{\mathbf{q}}$, $\beta_{\mathbf{q}}$, $\alpha_{\mathbf{q}}$) and ($\eta^+_{\mathbf{q}}$, $\gamma^+_{\mathbf{q}}$, $\eta_{\mathbf{q}}$, $\gamma_{\mathbf{q}}$) are Fermi operators, and $\lambda_{\mathbf{q}}^{\rm AF}$ and $\lambda_{\mathbf{q}}^{\rm CAF}$ are eigenvalues of the corresponding matrices in formulas (15) and (16), which are determined as follows:

$$\lambda_{\mathbf{q}}^{\rm AF}(m_A^{\rm AF}) = \Big[(J_1 \cos q_y)^2 + (J_1' \sin q_x)^2 + + (-2\tilde{J} m_A^{\rm AF} + 2J_2 \cos q_x \sin q_y)^2\Big]^{1/2}, \quad (19)$$

$$\lambda_{\mathbf{q}}^{\rm CAF}(m_A^{\rm CAF}) = \Big[(J_1 \cos q_y)^2 + (2J_2 \sin q_x \sin q_y)^2 + + (2\tilde{J}' m_A^{\rm CAF} - J_1' \cos q_x)^2\Big]^{1/2}. \quad (20)$$

Hence, we reduced our problem to a problem of the ideal gas of fermions with the variational parameters $m_A^{\rm AF}$ and $m_A^{\rm CAF}$. The latter are determined from the condition of the minimum of the Helmholtz free energy. On the basis of Eqs. (17) and (18), we obtain the ground-state energy per site, in the thermodynamic

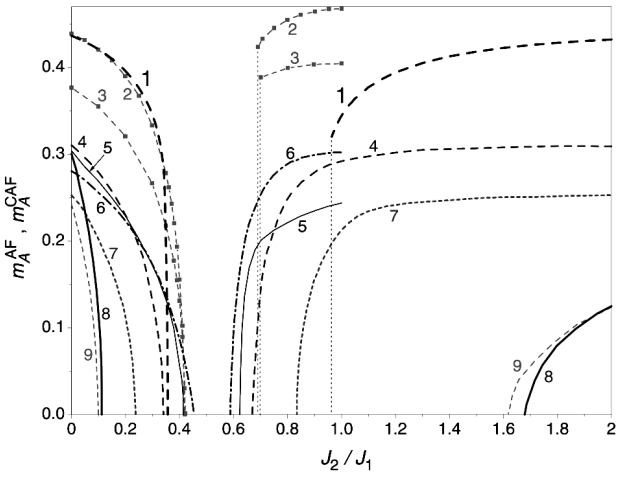

Fig. 2. Dependences of sublattice magnetizations on the parameter J_2/J_1 at $J_1' = J_1$ obtained in various approaches: our calculations (*1*); four-particle-cluster approximation [24] (*2*), sixteen-particle-cluster approximation [24] (*3*), finite-size scaling of exact diagonalization data [33] (*4*), density-matrix renormalization group method [18] (*5*), extrapolation of the data of coupled-cluster method [29] (*6*), and methods based on Green's functions: [26] (*7*), [27] (*8*), and [28] (*9*)

limit, for the case of different antiferromagnetic orderings,

$$\frac{E_0^{\rm AF}}{N_x N_y} = -\int\limits_{-\pi}^{\pi} \frac{{\rm d}q_x}{2\pi} \int\limits_{-\pi+|q_x|}^{\pi-|q_x|} \frac{{\rm d}q_y}{2\pi} \lambda_{\mathbf{q}}^{\rm AF} + \tilde{J}(m_A^{\rm AF})^2 =$$

$$= -\frac{1}{2}\int\limits_{-\pi}^{\pi} \frac{{\rm d}q_x}{2\pi} \int\limits_{-\pi}^{\pi} \frac{{\rm d}q_y}{2\pi} \lambda_{\mathbf{q}}^{\rm AF} + \tilde{J}(m_A^{\rm AF})^2, \qquad (21)$$

$$\frac{E_0^{\rm CAF}}{N_x N_y} = -\int\limits_{-\pi}^{\pi} \frac{{\rm d}q_x}{2\pi} \int\limits_{0}^{\pi} \frac{{\rm d}q_y}{2\pi} \lambda_{\mathbf{q}}^{\rm CAF} - \tilde{J}'(m_A^{\rm CAF})^2. \qquad (22)$$

Here, the magnetizations of sublattices $m_A^{\rm AF}$ and $m_A^{\rm CAF}$ are determined from the minimum conditions for $E_0^{\rm AF}(m_A^{\rm AF})$ and $E_0^{\rm CAF}(m_A^{\rm CAF})$, respectively.

3. Results of Numerical Calculations and Conclusions

Let us first consider the results of numerical calculations for the ground state in the case of spatially isotropic model ($J_1 = J_1'$). In Fig. 2, the dependences of the sublattice magnetization on the frustration parameter J_2/J_1, which were obtained on the basis of Eqs. (21) and (22), are depicted. Here, for the sake of comparison, we also present results from other works [18, 24, 26–29, 33]. The left curves correspond to the Néel antiferromagnetic ordering, and the right ones to the collinear stripe antiferromagnetic ordering.

First of all, we note that the results of such numerical approaches as the density-matrix renormalization group method [18] and the finite-size scaling of exact diagonalization data [33], as well as the data calculated in the coupled-cluster method [29], are in rather good agreement with each other. In particular, they provide well-consistent, at the quantitative level, values for the transition points J_2^{c1}/J_1 and J_2^{c2}/J_1, $m_A^{\rm AF}$-values that are close to each other at small values of frustration parameter ($J_2/J_1 \ll \ll J_2^{c1}/J_1$), and $m_A^{\rm CAF}$-values that are rather close to each other at large frustration parameter values ($J_2/J_1 \gg J_2^{c2}/J_1$). A shortcoming of those methods is the fact that they cannot reliably predict the order of phase transition. The results of many numerical approaches [16, 22, 32, 61–64] testify that the order parameter jumps to zero at the point J_2^{c2}/J_1, i.e. the quantum phase transition from the collinear antiferromagnetic ordering to the quantum paramagnetic (QP) one is of the first order. This conclusion is also confirmed by a drastic vanishing of $m_A^{\rm CAF}$ in a vicinity of J_2^{c2}/J_1, together with a reduction of the parameter J_2/J_1 given by the coupled-cluster method [29]. It should also be mentioned that the results of exact diagonalization with $N_x N_y = 40$, which were obtained in the recent work [32], differ insignificantly from the data in work [33] (see Fig. 2) obtained in a similar approach with a smaller maximum number of sites.

The results obtained in the framework of the methods on the basis of Green's functions [26–28], cluster approximation [24], and variational approach (see work [25]; its result is not shown in Fig. 2, because it is very close to the result of the four-particle-cluster approximation), as well as our results, are somewhat different from those obtained in works [18, 29, 33]. For instance, the variational method [25] and the approximation on the basis of four- and sixteen-particle clusters [24] predict too large values for $m_A^{\rm AF}$ at $J_2/J_1 \ll \ll J_2^{c1}/J_1$ and $m_A^{\rm CAF}$ at $J_2/J_1 \gg J_2^{c2}/J_1$, similarly to what takes place in our approximation. However, those three approaches assume that the phase transition between the quantum paramagnet and the collinear antiferromagnet is of the first order, which agrees, as was mentioned above, with the results of many researches. In addition, the cluster approxima-

tion and the variational method also predict rather good values for J_2^{c1}/J_1 and J_2^{c2}/J_1.

At the same time, the approaches on the basis of Green's functions, which were applied in works [27, 28], unlike the approach used in work [26], predict very imprecise values for the transition points J_2^{c1}/J_1 and J_2^{c2}/J_1. They also predict a too slow decrease of m_A^{CAF} to zero in a vicinity of the second phase transition (with a reduction of J_2/J_1 at $J_2/J_1 \gtrapprox J_2^{c2}/J_1$). The advantage of the results of those approaches in comparison with our ones consists in a substantially slower decrease of m_A^{AF} with the growth of J_2/J_1 in a vicinity of the left phase transition (at $J_2/J_1 \lessapprox J_2^{c1}/J_1$). In addition, in work [27], a rather precise value of m_A^{AF} was obtained for the non-frustrated ($J_2 = 0$) model.

Let us consider now the results of numerical calculations for the spatially anisotropic model ($J_1'/J_1 \neq \neq 1$), which we carried out on the basis of relations (21) and (22). In Fig. 3, the dependences of sublattice magnetizations in the ground state on the frustration parameter J_2/J_1 are depicted for various values of spatial anisotropy J_1'/J_1. Here again, the left curves correspond to the Néel antiferromagnetic ordering, and the right ones to the collinear stripe antiferromagnetic ordering. It is clear that the phase transition points were determined by comparing the energy of the system in different phases. The results of calculations are summarized in the phase diagram of the ground state exhibited in Fig. 4.

At large J_1'/J_1-values, when the ratio J_2/J_1 increases, the system undergoes two phase transitions: first, the transition of the second order from the Néel antiferromagnetic phase into the magnetically disordered one and, afterward, the transition of the first order from the disordered phase into the antiferromagnetic stripe one. At small values of J_1'/J_1 as J_2/J_1 increases we observe only one phase transition of the first order from antiferromagnetic Néel phase to the antiferromagnetic stripe one with the magnetizations of sublattices in vicinities of phase transition points, being distinct from zero both in the Néel and stripe phases.

Now, let us briefly mention the results of other methods that are known to us. Note at once that they differ qualitatively both from the ours and from one another. For instance, in the coupled-cluster method [54], if the J_1'/J_1-values are large, there are also two phase transitions as the parameter J_2/J_1 grows:

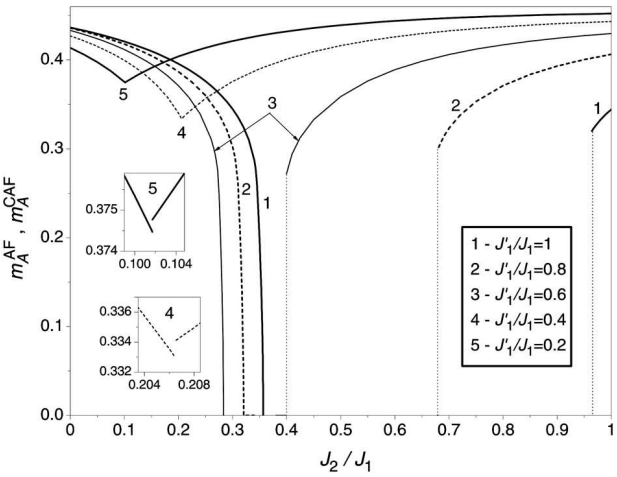

Fig. 3. Dependences of sublattice magnetizations on the frustration parameter J_2/J_1 at various values of spatial anisotropy parameter $J_1'/J_1 = 1$ (*1*), 0.8 (*2*), 0.6 (*3*), 0.4 (*4*), and 0.2 (*5*). Left curves correspond to the Néel ordering, and right ones to the stripe-like ordering

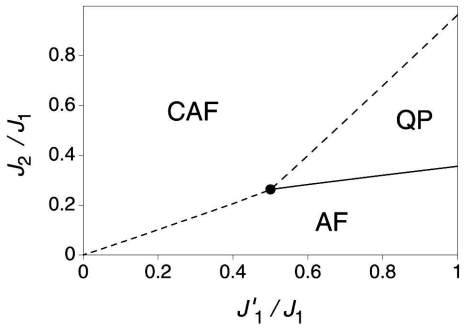

Fig. 4. Phase diagram of the ground state. The solid curve corresponds to the phase transition of the second order, and the dashed one to the phase transition of the first order

Néel antiferromagnetic phase → quantum paramagnet → stripe antiferromagnetic phase. However, the both transitions are assumed to be continuous. At small J_1'/J_1-values, the coupled-cluster method predicts one phase transition, as we do. However, in a vicinity of the phase transition point, the magnetizations of sublattices tend to zero both to the left (in the Néel antiferromagnetic phase) and to the right (in the collinear stripe phase).

In the framework of the variational method applied in work [53], the result obtained for large J_1'/J_1 is in qualitative agreement with our results (the lower phase transition is of the second order, and the upper one of the first order). However, at small values of the

spatial anisotropy parameter, the result differs qualitatively both from our results and from the result of the coupled-cluster method: in a vicinity of the single phase transition, the sublattice magnetization in the Néel antiferromagnetic phase tends to zero (as in the coupled-cluster method), whereas, in the antiferromagnetic stripe phase, it is different from zero (as in our method).

The result obtained in the spin-wave approach [49] considerably differs from all mentioned above. Namely, at any J_1'/J_1-values, two phase transitions are predicted with the growth of parameter J_2/J_1: Néel antiferromagnetic phase $\rightarrow$ magnetically disordered phase $\rightarrow$ stripe antiferromagnetic phase, with both transitions being of the second order. Therefore, in the phase diagram for the ground state obtained in the spin-wave approximation, there is no ternary point, which is characteristic of the mean-field approximation. This inconsistency follows from the fact that the spin-wave expansion is inexact near the phase transition, so that there arise artifacts in the magnetization behavior [49]. This circumstance makes the determination of the critical point problematic in this approximation.

Hence, the results obtained in this work give us ground to assert that the simple approximation of the mean-field type, which was used by us in the framework of the Jordan–Wigner transformation method, makes it possible to qualitatively describe the properties of the ground state in the frustrated spin-1/2 $J_1-J_1'-J_2$ Heisenberg models on a square lattice at a low spatial anisotropy ($J_1/J_1' \approx 1$). In the opposite case of strong spatial anisotropy, the issue concerning the applicability of the mentioned approach remains open, because different methods predict qualitatively different results. Moreover, we would like to emphasize that, in order to obtain quantitatively exact results in the framework of the fermionization approach, the correlations at the neighbor sites have to be taken into account self-consistently. This task will be a subject of our further research.

1. P. Carretta, N. Papinutto, C.B. Azzoni, M.C. Mozzati, E. Pavarini, S. Gonthier, and P. Millet, Phys. Rev. B **66**, 094420 (2002).
2. R. Melzi, P. Carretta, A. Lascialfari, M. Mambrini, M. Troyer, P. Millet, and F. Mila, Phys. Rev. Lett. **85**, 1318 (2000).
3. R. Melzi, S. Aldrovandi, F. Tedoldi, P. Carretta, P. Millet, and F. Mila, Phys. Rev. B **64**, 024409 (2001).
4. P. Carretta, R. Melzi, N. Papinutto, and P. Millet, Phys. Rev. Lett. **88**, 047601 (2002).
5. H. Rosner, R.R.P. Singh, W.H. Zheng, J. Oitmaa, and W.E. Pickett, Phys. Rev. B **67**, 014416 (2003).
6. A. Bombardi, J. Rodriguez-Carvajal, S. Di Matteo, F. de Bergevin, L. Paolasini, P. Carretta, P. Millet, and R. Caciuffo, Phys. Rev. Lett. **93**, 027202 (2004).
7. E.E. Kaula, H. Rosnera, N. Shannonb, R.V. Shpanchenkoc, and C. Geibel, J. Magn. Magn. Mater. **272–276**, 922 (2004).
8. M. Skoulatos, J.P. Goff, C. Geibel, E.E. Kaul, R. Nath, N. Shannon, B. Schmidt, A.P. Murani, P.P. Deen, M. Enderle, and A.R. Wildes, Europhys. Lett. **88**, 57005 (2009).
9. M. Inui, S. Doniach, and M. Gabay, Phys. Rev. B **38**, 6631 (1988).
10. P. Chandra and B. Doucot, Phys. Rev. B **38**, 9335 (1988).
11. E. Dagotto and A. Moreo, Phys. Rev. Lett. **63**, 2148 (1989).
12. G. Misguich and C. Lhuillier, in *Frustrated Spin Systems* (World Scientific, Singapore, 2013), p. 235.
13. D. Poilblanc, E. Gagliano, S. Bacci, and E. Dagotto, Phys. Rev. B **43**, 10970 (1991).
14. L. Capriotti and S. Sorella, Phys. Rev. Lett. **84**, 3173 (2000).
15. L. Capriotti, F. Becca, A. Parola, and S. Sorella, Phys. Rev. Lett. **87**, 097201 (2001).
16. T. Li, F. Becca, W. Hu, and S. Sorella, Phys. Rev. B **86**, 075111 (2012).
17. L. Wang, Z.-C. Gu, F. Verstraete, and X.-G. Wen, arXiv:1112.3331 [cond-mat.str-el].
18. H.C. Jiang, H. Yao, and L. Balents, Phys. Rev. B **86**, 024424 (2012).
19. F. Mezzacapo, Phys. Rev. B **86**, 045115 (2012).
20. W.-J. Hu, F. Becca, A. Parola, and S. Sorella, Phys. Rev. B **88**, 060402(R) (2013).
21. S.S. Gong, W. Zhu, D.N. Sheng, O.I. Motrunich, and M.P.A. Fisher, Phys. Rev. Lett. **113**, 027201 (2014).
22. S. Morita, R. Kaneko, and M. Imada, J. Phys. Soc. Jpn. **84**, 024720 (2015).
23. L. Balents, Nature (London) **464**, 199 (2010).
24. Y.-Z. Ren, N.-H. Tong, and X.-C. Xie, J. Phys.: Condens. Matter **26**, 115601 (2014).
25. M.J. de Oliveira, Phys. Rev. B **43**, 6181 (1991).
26. L. Siurakshina, D. Ihle, and R. Hayn, Phys. Rev. B **64**, 104406 (2001).
27. A.F. Barabanov and V.M. Berezovsky, Phys. Lett. A **186**, 175 (1994).
28. A.F. Barabanov, A.V. Mikheenkov, and A.V. Shvartsberg, Teor. Mat. Fiz. **168**, 389 (2011).
29. J. Richter, R. Zinke, and D.J.J. Farnell, Eur. Phys. J. B **88**, 2 (2015).
30. O. Götze, S.E. Krüger, F. Fleck, J. Schulenburg, and J. Richter, Phys. Rev. B **85**, 224424 (2012).
31. R. Darradi, O. Derzhko, R. Zinke, J. Schulenburg, S.E. Krüger, and J. Richter, Phys. Rev. B **78**, 214415 (2008).

32. J. Richter and J. Schulenburg, Eur. Phys. J. B **73**, 117 (2010).
33. H.J. Schulz, T.A.L. Ziman, and D. Poilblanc, J. Phys. I (Paris) **6**, 675 (1996).
34. O. Derzhko, J. Phys. Stud. **5**, 49 (2001).
35. E. Lieb, T. Schultz, and D. Mattis, Ann. Phys. (N.Y.) **16**, 407 (1961).
36. M.C. Chang and M.F. Yang, Phys. Rev. B **66**, 184416 (2002).
37. O. Derzhko, T. Verkholyak, R. Schmidt, and J. Richter, Physica A **320**, 407 (2003).
38. O. Derzhko and T. Krokhmalskii, Physica B **337**, 357 (2003).
39. D.C. Cabra and G.L. Rossini, Phys. Rev. B **69**, 184425 (2004).
40. O. Derzhko and T. Krokhmalskii, Czech. J. Phys. **55**, 601 (2005).
41. P. Lou, Phys. Rev. B **72**, 064435 (2005).
42. T. Verkholyak, A. Honecker, and W. Brenig, Eur. Phys. J. B **49**, 283 (2006).
43. T. Verkholyak, J. Strečka, M. Jaščur, and J. Richter, Eur. Phys. J. B **80**, 433 (2011).
44. S. Paul and A.K. Ghosh, J. Magn. Magn. Mater. **362**, 193 (2014).
45. K. Kumar, K. Sun, and E. Fradkin, Phys. Rev. B **90**, 174409 (2014).
46. A.A. Nersesyan and A.M. Tsvelik, Phys. Rev. B **67**, 024422 (2003).
47. A.A. Tsirlin and H. Rosner, Phys. Rev. B **79**, 214417 (2009).
48. O. Volkova, I. Morozov, V. Shutov, E. Lapsheva, P. Sindzingre, O. Cépas, M. Yehia, V. Kataev, R. Klingeler, B. Büchner, and A. Vasiliev, Phys. Rev. B **82**, 054413 (2010).
49. K. Majumdar, Phys. Rev. B **82**, 144407 (2010).
50. K. Majumdar, D. Furton, and G.S. Uhrig, Phys. Rev. B **85**, 144420 (2012).
51. S. Moukouri, J. Stat. Mech. Theor. Exp. **2006**, P02002 (2006).
52. G. Mendonça, R. Lapa, J.R. de Sousa, M.A. Neto, K. Majumdar, and T. Datta, J. Stat. Mech. Theor. Exp. **2010**, P06022 (2010).
53. O.D. Mabelini, O.D.R. Salmon, and J. Ricardo de Sousa, Solid State Commun. **165**, 33 (2013).
54. R.F. Bishop, P.H.Y. Li, R. Darradi, and J. Richter, J. Phys.: Condens. Matter **20**, 255251 (2008).
55. P. Sindzingre, Phys. Rev. B **69**, 094418 (2004).
56. Y. R. Wang, Phys. Rev. B **43**, 3786 (1991).
57. O.R. Baran and T.M. Verkholyak, preprint ICMP-15-01U (2015).
58. O.R. Baran and T.M. Verkholyak, preprint ICMP-15-05U (2015).
59. Y.R. Wang, Phys. Rev. B **46**, 151 (1992).
60. G. Misguich, Th. Jolicoeur, and S.M. Girvin, Phys. Rev. Lett. **87**, 097203 (2001).
61. H.J. Schulz and T.A.L. Ziman, Europhys. Lett. **18**, 355 (1992).
62. Z. Fan and Q.-L. Jie, Phys. Rev. B **91**, 195118 (2015).
63. J.-F. Yu and Y.-J. Kao, Phys. Rev. B **85**, 094407 (2012).
64. C.-P. Chou and H.-Y. Chen, Phys. Rev. B **90**, 041106(R) (2014).

Received 24.11.15.
Translated from Ukrainian by O.I. Voitenko

О.Р. Баран, Т.М. Верхоляк

ДВОВИМІРНА СПІН-1/2 $J_1 - J_1' - J_2$
МОДЕЛЬ ГАЙЗЕНБЕРҐА В РАМКАХ
ПЕРЕТВОРЕННЯ ЙОРДАНА–ВІҐНЕРА

Р е з ю м е

Для просторово анізотропної спін-1/2 моделі Гайзенберґа на квадратній ґратці з антиферомагнітними взаємодіями між найближчими та наступними після найближчих сусідами використано перетворення Йордана–Віґнера і отримано гамільтоніан безспінових ферміонів, що перестрибують між сусідніми вузлами у калібрувальному полі. В результаті наближення типу середнього поля для фазових множників (що відповідають калібрувальному полю), а також для прямої взаємодії між ферміонами, задача зведена до вільного газу Фермі. Розглянуто два можливі типи антиферомагнітних впорядкувань (Нееля та колінеарне), обчислено енергії основного стану і на основі цього досліджено квантові фазові переходи, зумовлені фрустрацією взаємодій.